Local structure of ternary ordering Cu-Zn-Al alloy and thermo-elastic martensitic transformation

1989 J. Phys.: Condens. Matter 1 2581

(http://iopscience.iop.org/0953-8984/1/15/004)

J. Phys.: Condens. Matter 1 (1989) 2581–2592. Printed in the UK

Local structure of ternary ordering Cu–Zn–Al alloy and thermo-elastic martensitic transformation

T Girardeau†, J Mimault† and C Mai‡

† Métallurgie Physique (Unitée associée au CNRS 131), 40 avenue du Recteur Pineau 86022, Poitiers, France

‡ Groupe d'Etudes de Métallurgie Physique et de Physique des Matériaux (Laboratoire associé au CNRS 341), 20 avenue A. Einstein 69621, Villeurbanne, France

Received 12 July 1988, in final form 14 October 1988

Abstract. Extended x-ray absorption fine-structure (EXAFS) studies have been performed, in transmission mode, on $Cu_{68}Zn_{15}Al_{17}$ brass using the synchrotron radiation facility at Laboratoire d'Utilisation du Rayonnement Electromagnétique. The spectra have been recorded at the Cu K and Zn K edges for different temperatures around the martensitic transformation temperature domain. The study of the temperature dependence of the Cu and Zn surroundings provides two main pieces of information.

(i) The pure Cu sublattice deviates from the virtual crystal and absorbs the local stresses owing to the different sizes of the Zn, Cu and Al atoms which constitute the second sublattice; this behaviour is similar to that of ternary semiconducting random solid solutions such as $In_xGa_{1-x}As$ or $Cd_xHg_{1-x}Te$.

(ii) Zn and Cu neighbour environments evolve differently as the martensitic transformation takes place. In particular, around the Zn atoms, a lengthening of the atomic distances is observed only for premartensitic domain temperatures. The Cu K spectra evolve more gradually and an increase in the nearest-neighbour distances is observed during the whole transformation.

1. Introduction

Alloys which have undergone martensitic transformation have been extensively studied for their shape-memory effect; of this material family, β-brass alloys are certainly one of the most investigated groups in which the thermo-elastic transformation is reversible with a weak hysteresis with respect to temperature. Much information has been collected by means of TEM (Chakravorty and Wayman 1977, Van Tendeloo *et al* 1986) or x-ray diffraction experiments (Scarsbrook *et al* 1984) which generally conclude, for Cu–Zn–Al alloys, 18R (martensitic phase) and DO_3 (parent phase) structures. The crystalline parameters have been well described and a premartensitic effect evidenced before the nucleation process. Nevertheless, Bragg scattering is averaged over many unit cells and, except for the diffuse background which is difficult to collect and analyse, no information can be extracted about any specific movement of one atomic species during the transformation; other experiments such as differential scanning calorimetry have provided an empirical relation between the temperature M_s (the start of martensitic nucleation) and the Zn concentration and one could investigate the role played by each type of atom in the start of nucleation. The EXAFS technique is well suited to obtaining information

0953-8984/89/152581 + 12 $02.50

about this point; its local character and its chemical sensitivity (Lee *et al* 1981) enable investigations of the lattice distortions around each atom type to be made. The EXAFS signal analysis provides structural local information about the first shells surrounding the excited atoms, which are selected according to their chemical nature.

We report, in this paper, an EXAFS study of a Cu–Zn–Al foil during its cooling from 300 to 30 K. Cu K and Zn K edge spectra have been recorded at different stages of the cooling. To make judicious use of the inverse back-scattering properties of the Al atoms with respect to those of the Cu and Zn atoms, a sufficiently high Al atomic concentration was necessary. In contrast, the collection of the correct data for both Cu and Zn atoms required a similarly sufficiently high Zn atomic concentration. As the Cu percentage remains close to 68 at.% in this brass family, $Cu_{68}Zn_{15}Al_{17}$ was used for this EXAFS study.

First, we describe the experimental conditions and verify that the collected signals are not damped by any thickness effect. After summarising the expected atomic environments, we qualitatively comment on the apparent characteristics of the spectrum and its evolution during cooling. Then the EXAFS analysis process is briefly recalled and quantitative simulations are performed to extract the different atomic pair distances according to their chemical nature. Finally, we discuss the similarity between the lattice distortions measured for the present material and those for ternary semiconductor solid solutions.

2. X-ray measurements and data reduction

X-ray absorption measurements were performed in the transmission mode at the Laboratoire d'Utilisation du Rayonnement Electromagnétique (LURE), using the synchrotron radiation source. An Si(220) channel-cut x-ray monochromator delivered the monochromatic beam and the spectra were recorded from 150 eV below the Cu K threshold to 750 eV above the Zn K threshold. The sample was mounted in a cryostat equipped with a controlled temperature system. At every recording point, at least two consecutive data points were collected for the same signal and later added for analysis. As explained further, the cooling was planned first to measure the pure parent phase, then to follow the local lattice parameter variation during martensitic transformation and finally to reach the pure martensitic phase.

The sample thickness was adjusted to obtain reasonable edge steps for both Cu K and Zn K absorption and the chosen concentration requires a 25 μm thickness to attain such results. As illustrated in figure 1, these experimental conditions yield nevertheless a significant Cu K edge step and a weak edge for Zn K absorption:

$$\Delta\mu_{Cu}\, x_{Cu} t = 2.2 \qquad \Delta\mu_{Zn}\, x_{Zn} t = 0.5$$

where t is the foil thickness, x the atomic concentration and $\Delta\mu$ the unitary specific K-edge step.

According to Stern and Kim (1981), the large edge steps can be damped by pinholes in the sample or harmonic radiation in the incoming beam. Consequently the EXAFS signal may be attenuated and distorted; so, before analysing the spectra, we have to verify the importance of this amplitude leakage. Starting with the MacMasters Cu K and Zn K absorption step values, the experimental results easily provide relative Cu and Zn concentrations and thicknesses. Calculations yield 67 at.% Cu and 15 at.% Zn and starting with the Cu or the Zn edge steps, the calculated thicknesses coincide. A thickness effect on such disproportionate edge steps cannot yield identical damping except in an

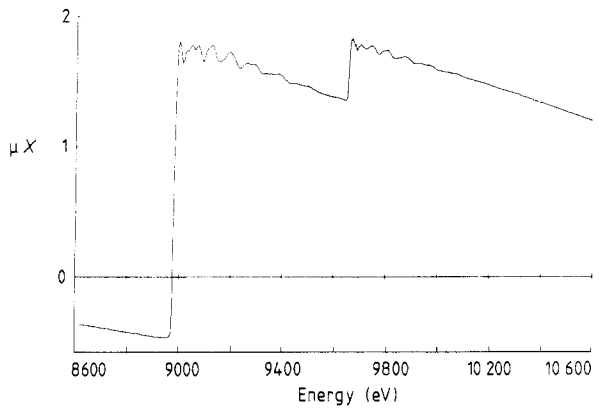

Figure 1. Raw absorption data in energy space for $Cu_{68}Zn_{15}Al_{17}$ foil.

unfortunately random way; so we conclude that there is an insignificant thickness effect and that the weak EXAFS Cu K amplitudes can be analysed with confidence.

After removal of the absorption signal background and normalisation of the observed oscillations relative to the edge step, the EXAFS signal is Fourier transformed to provide a real-space spectrum. As shown in the example in figure 2, this distance distribution function presents a single main peak situated at around the first-shell distance. In order to analyse its EXAFS, this peak is isolated and then back Fourier transformed. The whole process is detailed in a previous paper (Mimault *et al* 1981). Figure 2 principally shows the Zn K and Cu K spectra obtained at 130 K, a martensitic domain temperature. In the same figure, dotted curves correspond to the signals obtained at a temperature higher than M_S, 160 K, before martensitic transformation occurs.

3. Expected local structures and EXAFS spectrum behaviour

Before the spectra analysis, we recall the main crystallographic structures which have been reported in literature on parent and martensitic phases.

TEM experiments (Rapacioli and Alhers 1977) on the $Cu_{68}Zn_{15}Al_{17}$ (or a very similar composition) specimen show clearly that martensitic transition transforms a DO_3 structure to an 18R one. This sample is characterised by a BCC lattice parameter a_β of 5.996 Å (Chakravorty and Wayman 1977) and the following lattice parameters for martensitic structures (Scarsbrook *et al* 1984): $a = 4.553$ Å, $b = 5.452$ Å, $c = 38.97$ Å and $\beta = 87.5°$ (a and b are the lattice parameters of the basal planes and c is the 'perpendicular' stacking periodic distance). The stacking positions of the basal plane deviate from their ideal positions (Chakravorty and Wayman 1977) of $a/3$ and $2a/3$ to $a/2.73$ and $2a/2.73$ positions. This correction provides uniformity of the first-shell distance distribution.

Because of the quenching temperature used in the sample elaboration, this specimen was often found to be (Rapacioli and Alhers 1977) a mixture of B2 and DO_3 crystallites, above the martensitic temperature M_s. The long-range order in Cu–Zn–Al alloys has been detailed by Rapacioli and Alhers (1979). The B2 structure is described as two sublattices: one is wholly occupied by the Cu atoms while the Zn, Al and remaining Cu atoms ($x_{Cu} > 0.5$) are randomly distributed on the other sublattice. The DO_3 order acts on this mixed sublattice in such a way that Cu–Al next-nearest-neighbour pairs are more numerous. Martensitic transformation is known to be diffusionless and therefore the

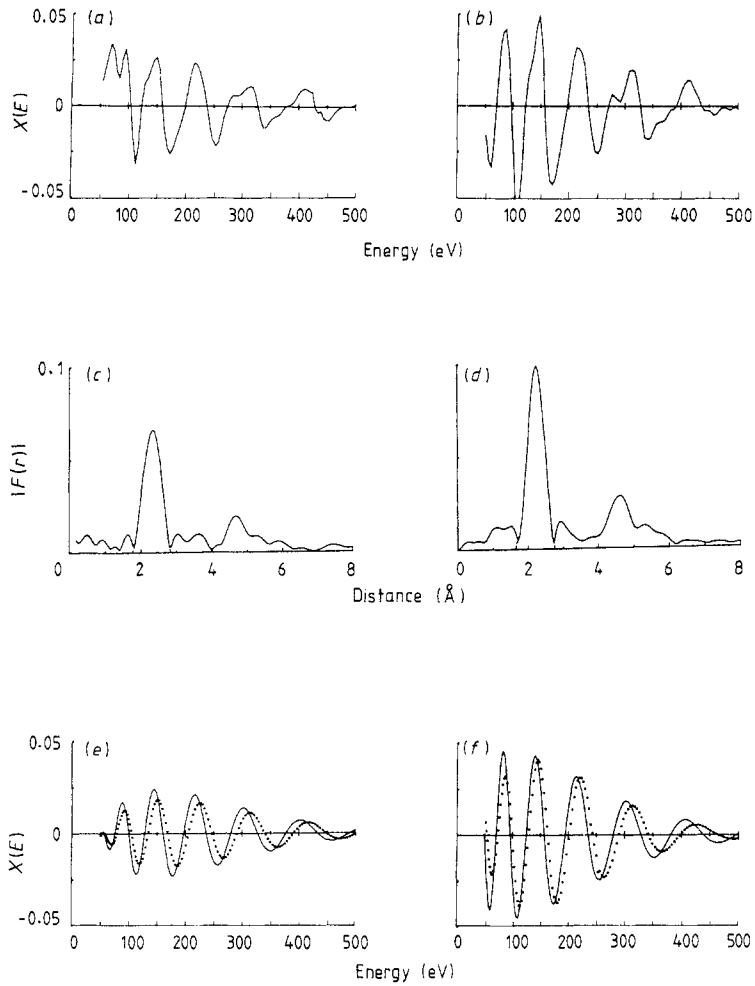

Figure 2. (*a*), (*b*) Raw data in *k*-space after background substraction, (*c*), (*d*) Fourier transform of data from (*a*) and (*b*) and (*e*), (*f*) retransformed data from (*c*) and (*d*) after filtering the main peak for (*a*), (*c*), (*e*) the Cu K edge and (*b*), (*d*), (*f*) the Zn K edge: ——, 140 K data; · · · , 190 K data.

martensitic phase (M18R or M9R) inherits the chemical order of the parent phase. Within this framework, the Cu and Zn average atomic environments of the idealised DO_3/M18R/M9R/B2 structures have been estimated (table 1).

As evidenced, the B2 and DO_3 environments are very similar for each central atom type; the EXAFS analysis cannot detect such insignificant differences. The same conclusion is naturally assumed for 9R or 18R structures.

Small differences exist only in the second-shell compositions, and they are still minimised (Rapacioli and Alhers 1979) by short-range chemical disorder which may remain, according to the quenching rate used.

We can nevertheless emphasise the following points about the number of neighbours and their distances from the excited atoms.

Table 1. Average number of Cu and Zn atoms in various locations.

	Martensitic phase			BCC (parent) phase		
Central atom	Phase structure	First shell, $d_1 = 2.63$ Å	Second shell, $d_2 = 2.73$ Å	Phase structure	First shell, $d_1 = 2.59$ Å	Second shell, $d_2 = 2.99$ Å
Cu	M18R	4 Cu, 2 Al, 2 Zn	3 Cu, 0.3 Zn, 0.7 Al	DO_3	4 Cu, 2 Al, 2 Zn	4.5 Cu, 0.5 Zn, 1 Al
Cu	M9R	4 Cu, 2 Al, 2 Zn	3.3 Cu, 0.3 Zn, 0.4 Al	B2	4 Cu, 2 Al, 2 Zn	5 Cu, 0.4 Zn, 0.6 Al
Zn	M18R	8 Cu	1.5 Cu, 1.2 Zn, 1.3 Al	DO_3	8 Cu	2.3 Cu, 1.8 Zn, 1.9 Al
Zn	M9R	8 Cu	1.4 Cu, 1.2 Zn, 1.4 Al	B2	8 Cu	2.1 Cu, 1.8 Zn, 2.1 Al

(i) First- and second-shell distances are too weakly separated to provide two different peaks. So, signals have to be analysed as the interference of the two contributions.

(ii) The first-shell composition does not vary during the whole experiment and a chemical discrepancy is expected between the Cu K and Zn K signals. Because of its uniformity, the first shell plays a preponderant role in the K–Zn spectrum and, consequently, the analysis might be straightforward to achieve. In contrast, the Cu K signal contains a mixture of Al, Cu and Zn atoms which partially destroys the constructive interference due to close distances. The second-shell distribution shows the opposite behaviour; the Cu next-nearest neighbours might give a significant EXAFS contribution, equivalent to the first-shell contribution to the Cu K signal.

Now, close examination of the experimental spectra in figure 2 (and particularly in figures 2(*e*) and 2(*f*)) yields immediately the following qualitative comments.

(i) Although different respective weights might be given to the contributions from the first and second shells, Cu and Zn signals present very similar k periodicities. This is particularly surprising for the parent phase where the two shells are separated by 0.40 Å; the interference effect might change spectacularly the spectra as the energy increases an a long-k wave interference might emerge from the Cu signal, but the experimental data do not behave in this way.

(ii) Comparison of the spectra before and after martensitic transformation shows a slight periodicity evolution which is characteristic of only the first-shell distance which increases as the sample cools. Additionally, although two next-nearest neighbours disappear, the back-scattering amplitude remains rather stable during the transformation.

Such behaviour suggests that large disorder affects the second-shell distance distribution during the whole experiment temperature range 30–220 K; consequently its origin cannot be only in the premartensitic effect as for a Cu–Zn specimen (Guénin and Gobin 1982). Before reporting the quantitative simulation of the signals and verifying these qualitative assumptions, we further recall the EXAFS simulation process.

4. Numerical analysis process

EXAFS signals have been analysed within the 100–500 eV range where a single-scattering model can be applied with confidence; the theoretical resulting expression (Lee *et al* 1981) which described this spectrum range is as follows:

$$\chi(k) = -\sum_{i=1}^{2}\sum_{n=1}^{3}\frac{N_{i,n}F_n(\pi,k)}{kR_{i,n}^2}\exp\left(-\frac{2R_{i,n}}{\lambda(k)}\right)\exp(-2\sigma_i^2k^2)\sin[2kR_{i,n}+\varphi_n(k)]$$

$$\hbar^2k^2/2m = (\hbar\omega - E_0).$$

k is the photo-electron wavevector; $N_{i,n}$ and $R_{i,n}$, respectively, are the atom number and the distance of the ith shell from the excited central atom; n indicates the chemical nature of the back-scatterer. E_0 is the threshold energy of the absorption edge. $\lambda(k)$, modelled as a g/k function, simulates the inelastic scattering as a photo-electron mean free path; g will be assigned as 4.5 eV as generally estimated in this kind of metallic material. To take account of the mean-square displacement about the average distance, a specific Debye–Waller term will be applied on each shell.

$\varphi_n(k)$ and $F_n(k)$ respectively, represent the total phase shift and back-scattering modulus experienced by the photo-electron during the absorption phenomenon. Some of these values, φ_{Cu-Cu}, φ_{Zn-Zn}, F_{Cu} and F_{Zn}, have been extracted from standard data (Girardeau *et al* 1988); the crossed phase shifts φ_{Cu-Zn} and φ_{Zn-Cu} have been estimated starting from the previous experimental values and subtracting or adding the theoretical back-scattering phase shift variation $\psi_{Cu} - \psi_{Zn}$ (Fontaine *et al* 1979) which provides, in this case, very small differences. ψ_n is the specific back-scatterer phase shift. All these parameters have been tested on the well known Cu–Zn martensitic structures (Girardeau *et al* 1988). The values of F_{Al}, φ_{Zn-Al} and φ_{Cu-Al} needed to analyse the data are obtained by theoretical calculation and were used in previous studies (Mimault *et al* 1981, Fontaine *et al* 1979). A comparison with the phase shifts obtained as previously by the operations

$$\varphi_{Cu-Al} = \varphi_{Cu-Cu} - (\psi_{Cu} - \psi_{Al})$$

$$\varphi_{Zn-Al} = \varphi_{Zn-Zn} - (\psi_{Zn} - \psi_{Al})$$

leads to very similar results for the highest-k range; they diverge only in a slight increase in the slope k which can lead to a variation in R of the order of 0.02 Å.

Fits are quantitatively adjusted by a least-squares technique applied on the zero-spectra location; the detailed process has been described elsewhere (Girardeau *et al* 1988). Qualitative comparison between experimental and simulated amplitudes allows us to distinguish between several good variance results or to modify the structure model in a correct way; it determines also the Debye–Waller term value.

5. Results and discussion

5.1. Martensitic structure

Operating with the expected chemical local environment, and using distances as free parameters (the starting values were those derived from x-ray diffraction experiments), we performed calculations on the Zn K and Cu K signals.

The Zn K results agree very well with the expected atomic distribution, including first- and second-shell surroundings; the amplitude fit was easily obtained. As shown in figure 3, the variance evolution is closely related to the first-neighbour Zn–Cu distance and a deep minimum is well developed within the narrow R range around 2.57 Å; so, the first-shell distance is determined rather precisely and the variance error bars can be estimated to be about 0.01 Å; the retained value is clearly shifted by −0.06 Å from the expected value. The mixed second-shell distance cannot be so accurate; it contributes weakly to the EXAFS signal and the variance minimum becomes large with respect to the next-nearest-neighbour distance. Nevertheless, the best fit is obtained for 2.72 Å, in conformity with the Bragg scattering results. As shown in figure 3, an excellent simulation is achieved, giving us confidence in the theoretical back-scattering amplitudes used, especially in the low-k range where the Al value is particularly important. The high-k range fits required a significant Debye–Waller term, 0.17 au, which is anomalously large for the operating temperature; this suggests (as previously concluded from the qualitative signal form) important static disorder which originates from local distortions of the lattice.

The Cu K signal, as presumed, does not agree completely with the total composition in table 1. The simulated spectra, and particularly amplitudes in the low-k range, appear

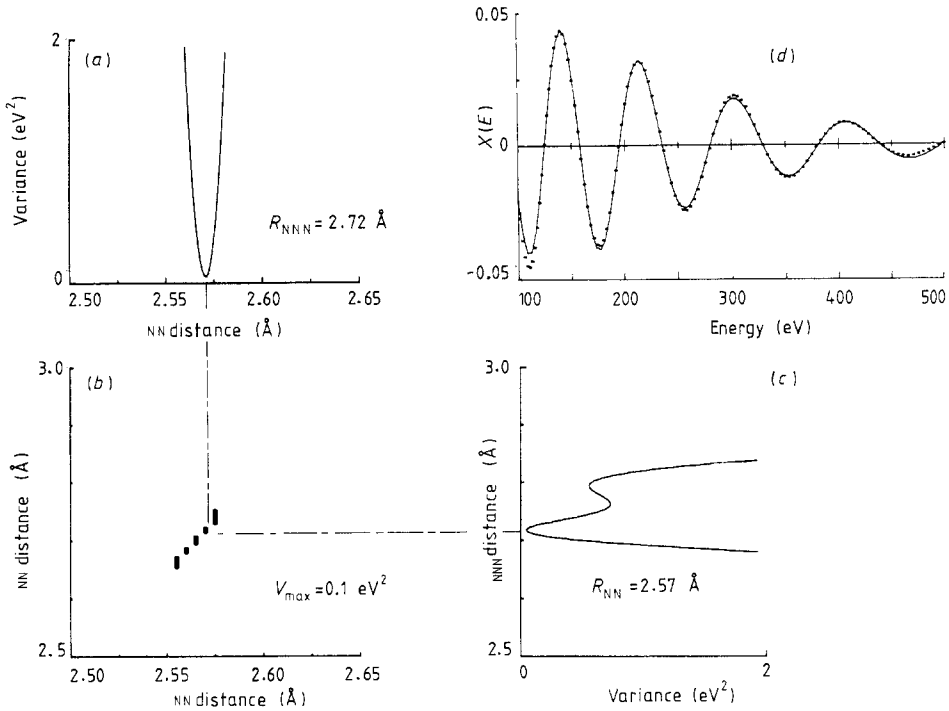

Figure 3. Results for Zn K edge spectrum (140 K; martensitic structure): (*a*) variance behaviour against nearest-neighbour distance; (*b*) solution in (R_{NN}, R_{NNN}) map; (*c*) variance behaviour with R_{NNN}; (*d*) spectra simulation (——, calculated signal; · · · , experimental signal).

to be too different from the experimental spectra to hope to achieve an improvement by slight variations in the planned environment parameters.

On the contrary, better agreement can easily be achieved with a significant damping of the second-shell weight. According to the Zn K threshold result, the Cu–Zn pairs are fixed at 2.57 Å and a variance procedure is applied to the Cu–Cu and Cu–Al nearest-neighbour distances. As shown in figure 4, the best fit leads to the following idealised values:

2 Zn at 2.57 ± 0.01 Å

4 Cu at 2.61 ± 0.01 Å

2 Al at 2.72 ± 0.03 Å.

Because there are a larger number of Cu–Cu pairs, this is adjusted by giving it a lower bar than for the Cu–Al pairs.

The Debye–Waller term needed to fit the amplitude of the signal has approximately the same value as that for the Zn K results and this is significant to the coherence of the model used.

In order to make the interpretation model homogeneous, some attempts have been made to simulate Zn K data with only the first-shell surrounding the central atom. Although a variance process does not yield a complete successful simulation of the EXAFS

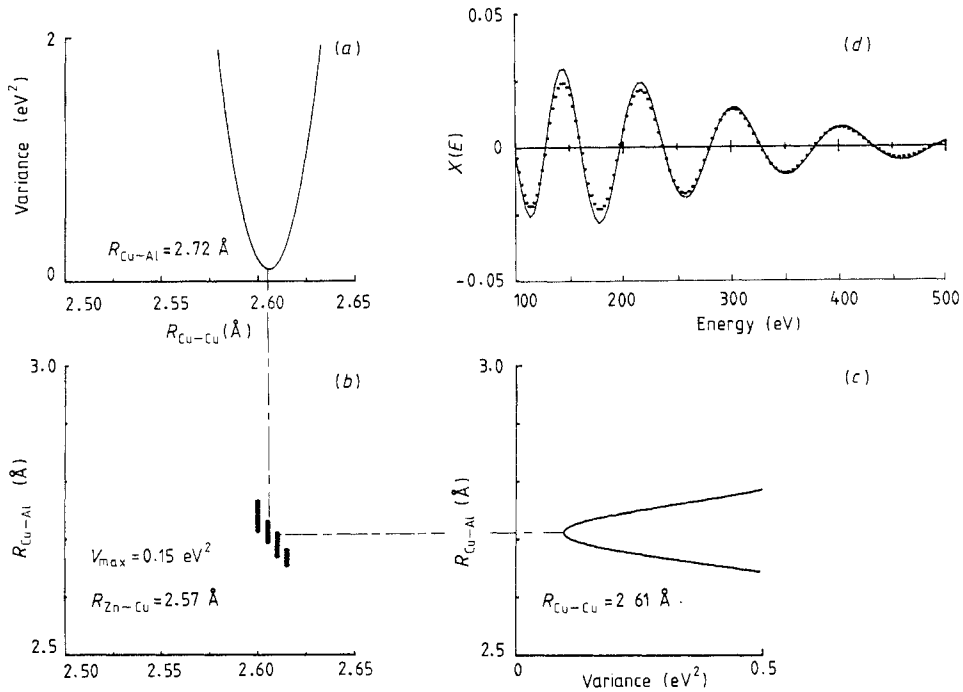

Figure 4. Results for Cu K edge spectrum (140 K): (*a*) variance behaviour with R_{Cu-Cu}; (*b*) solution area in $(R_{Cu-Al}, R_{Cu-Cu})_{NN}$ map; (*c*) variance behaviour with R_{Cu-Al}; (*d*) spectra simulation (——, calculated signal; · · · , experimental signal).

spectrum, the best fit is obtained with $R = 2.56$ Å; theoretical amplitudes are slightly, but not drastically, lower than the experimental ones. Such insensitivity to the second-shell back-scattering arises because of its chemical distribution.

5.2. Parent phase and martensitic transformation

The whole experimental set-up is summarised in figure 5(*a*). According to differential scanning calorimetry results, the $Cu_{68}Al_{17}Zn_{15}$ undergoes martensitic transformation in a restricted temperature range at around 160 K. So, it was planned to collect, first, data at some temperature points above this critical domain to obtain any information about premartensitic effects.

220 and 190 K data have been analysed with the BCC environment model; simulations appeared to be extremely inconsistent with the second-shell environments even when a high Debye–Waller term was introduced to take into account a low contribution. Good fits are only reached for both K-edge spectra when strictly only the first-shell environment is used. Such behaviour is not surprising if one considers the premartensitic effect as the development of $\{110\}\langle 1\bar{1}0\rangle$ displacement shear waves through the matrix (Guénin and Gobin 1982); it has no effect on the nearest-neighbour pairs which are in the perpendicular $\langle 111\rangle$ orientation. On the contrary, all the other pairs are greatly affected and their distance distribution is markedly broadened.

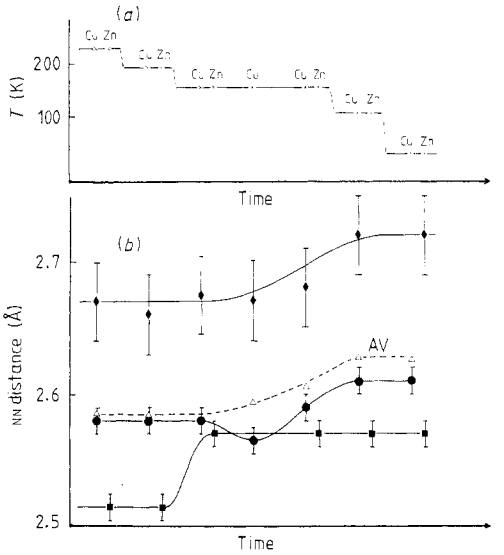

Figure 5. (*a*) Schematic representation of the routine used to collect the spectra during the cooling; (*b*) calculated nearest-neighbour distance (■, Zn–Cu pairs; ●, Cu–Cu pairs; ♦, Cu–Al pairs; △, average first-shell distance).

Coherent fits for both signals require a splitting of the bond length distribution, according to the chemical pair nature. The least-squares procedure yields the same results for 220 and 190 K experiments:

$$R_{\mathrm{Zn-Cu}} = 2.52 \pm 0.01 \text{ Å}$$

$$R_{\mathrm{Cu-Cu}} = 2.58 \pm 0.01 \text{ Å}$$

$$R_{\mathrm{Cu-Al}} = 2.67 \pm 0.03 \text{ Å}.$$

The observed spacings $R_{\mathrm{Cu-Cu}} - R_{\mathrm{Zn-Cu}}$ for the martensitic and the cubic phases are similar. Consequently, these spacings must originate from the different atomic sizes and the chemical ordering which arises in the Cu–Zn–Al structures.

The location of k nodes in the spectra begins to shift when temperature falls to 160 K. At this stage, as shown in figure 5(*a*), several successive spectra were collected, alternating their K-edge nature. The temperature control permitted us to maintain a constant temperature for only 2 h; we observed only a slight negative decrease of a few kelvins during this time. Surprisingly, the two K-edge spectra differ in their evolution as the experiment progresses. The node shift begins spectacularly in the Zn K spectrum and was achieved very rapidly. The Cu K spectrum shows a comparatively delayed and progressive evolution. All the data have been analysed with the first-shell composition which remains unchanged during the phase transformation. The distance results are summarised in figure 5(*b*); the curves drawn illustrate the different slopes of the time evolution around each atom species. The average first-neighbour distance is also shown (curve AV) and one can observe that the calculated values and the expected values coincide for each of the pure distinct phases.

5.3. Discussion

From EXAFS measurements on the Cu K and Zn K edges of the $Cu_{68}Zn_{15}Al_{17}$ sample, one can extract two main new pieces of information about the local matrix distortions and the asymmetric evolution of the Cu and Zn surroundings as the specimen structurally transforms.

First, experiments show a multi-model bond length distribution in this chemical ordered ternary alloy. Such behaviour has also been found for pseudo-binary alloys in covalently bonded materials (Mikkelsen and Boyce 1983, Balzarotti *et al* 1984) and ionically bonded alkali-halide solid solutions (Boyce and Mikkelsen 1983). In semiconductors such as $In_xGa_{1-x}As$ or $Cd_xHg_{1-x}Te$, the anion sublattice deviates from the virtual crystal and the mixed cation lattice more closely approximates it; the anion–cation pair distances are in a very small range around the distances observed in their corresponding binary compounds and remain quasi-insensitive to the concentration. The present results suggest that the division of the crystal in two sublattices provides a similar result. The pure Cu sublattice deviates from the virtual crystal and absorbs the local stresses due to the different sizes of the Zn, Cu and Al atoms constituting the second sublattice which correctly follows the virtual crystal structure. The extracted Cu–Zn distances are very close to those observed in binary Cu–39 at.% Zn which has the same crystalline structure (Girardeau 1988) (the B2 lattice gives 2.52 Å and the 9R lattice 2.57 Å). The Cu–Al nearest-neighbour pairs cannot be compared with any value observed for the same structure; nevertheless, the sum of Cu and Al radii gives 2.71 Å, a value which has been found in disordered Al–Cu substitution FCC alloys (Fontaine *et al* 1979). These conclusions can explain the lack of a second-neighbour EXAFS contribution, particularly at low temperatures on the Cu K edge; a Zn central atom makes the surrounding Cu cell contract while an Al central atom produces the opposite effect and would result in a large broadened distribution among the Cu–Cu next-nearest neighbours. Such local distortions are also certainly subject to the imperfect short-range chemical disorder which yields a rather dispersed distribution of the nearest-neighbour distance and can explain the relatively high Debye–Waller terms measured for the whole experiment.

Secondly, the particular evolution of the Cu–Zn nearest-neighbour distance relative to the other calculated parameters indicates that the cubic cells surrounding Zn atoms expand throughout the whole specimen in the early stages of the transformation. The martensitic thermo-elastic phenomenon is generally described (Guénin and Gobin 1978) as a gradual transformation of the matrix which begins at a temperature M_s and ends at a lower temperature M_f. The proportion of transformed parent phase is known to be a function of the temperature. The observed Cu nearest-neighbour parameters and the average inter-atomic distance seem to vary as follows: they may be considered to be the average of the two phases which coexist during the gradual evolution from a pure cubic structure sample to a pure martensitic sample. The volume of Zn nearest-neighbour cells surprisingly increase in a very limited temperature domain. Temperature control cannot be involved as the temperature was slightly but regularly decreased and the Zn environment remained stable outside this range. One can question whether the actual absolute distance is dependent on the phase shift or the energy spectra calibration used, but the relative distance variation cannot be questioned; a value of 0.05 Å completely agrees with the expected lattice parameter shift when the cubic phase is transformed to a martensitic phase. Such drastic temperature behaviour suggests that, first, local transformation strengthening processes take place around the Zn atoms and then this promotes macroscopic martensitic transformation.

Acknowledgments

The authors wish to thank A Fontaine for useful discussions of EXAFS spectra interpretation and the staff of LURE for help with the EXAFS measurements.

References

Balzarotti A, Czysyk M, Kisel A, Motta N, Podgorny M and Zimnal-Starnawska M 1984 *Phys. Rev.* B **30** 2895
Boyce J B and Mikkelsen J C 1983 *Bull. Am. Phys. Soc.* **28** 490
Chakravorty S and Wayman C M 1977 *Acta Metall.* **25** 989
Fontaine A, Lagarde P, Naudon A, Raoux D and Spanjaard D 1979 *Phil. Mag.* B **40** 17
Girardeau T, Mimault J, Mai Ch and Fontaine A 1988 *J. Phys. F: Met. Phys.* **18** 575
Guénin G and Gobin P F 1978 *Solid State Transformation in Metals Alloys* (Aussois: Editions de Physique) p 573
—— 1982 *Metall. Trans.* A **13** 1127
Lee P A, Citrin P H, Eisenberger P and Kincaid B M 1981 *Rev. Mod. Phys.* **53** 769
Mikkelsen J C Jr and Boyce J B 1983 *Phys. Rev.* B **28** 7130
Mimault J, Fontaine A, Lagarde P, Raoux D, Sadoc A and Spanjaard D 1981 *J. Phys. F: Met. Phys.* **11** 1311
Rapacioli R and Alhers M 1977 *Scr. Metall.* **11** 1147
—— 1979 *Acta Metall.* **27** 777
Scarsbrook G, Cook J M and Stobbs V W 1984 *Metall. Trans.* A **15** 1977
Stern E A and Kim K 1981 *Phys. Rev.* B **23** 3781
Van Tendeloo G, Chandrasekan M and Lovey F C 1986 *Metall. Trans.* A **17** 2153